Send Orders for Reprints to reprints@benthamscience.net

Medicinal Chemistry, **2019**, *15*, **521-536**

RESEARCH ARTICLE

Synthesis and Biological Evaluation of Polyfluoroalkylated Antipyrines and their Isomeric O-Methylpyrazoles

Natalya Agafonova[a], Evgeny Shchegolkov[*a], Yanina Burgart[a], Victor Saloutin[a], Alexandra Trefilova[b], Galina Triandafilova[b], Sergey Solodnikov[b], Vera Maslova[b], Olga Krasnykh[b], Sophia Borisevich[c] and Sergey Khursan[c]

[a]*Postovsky Institute of Organic Synthesis of the Ural Branch of the Russian Academy of Sciences, S. Kovalevskoy Str., 22, Ekaterinburg 620990, Russia;* [b]*Perm National Research Polytechnic University, Komsomolsky Av., 29, Perm 614990, Russia;* [c]*Ufa Institute of Chemistry of the Russian Academy of Sciences, Octyabrya Av., 71, Ufa 450078, Russia*

ARTICLE HISTORY

Received: March 30, 2018
Revised: October 19, 2018
Accepted: October 30, 2018

DOI:
10.2174/1573406414666181106145435

Abstract: ***Background:*** Formally belonging to the non-steroidal anti-inflammatory drug class pyrazolones have long been used in medical practices.

Objective: Our goal is to synthesize N-methylated 1-aryl-3-polyfluoroalkylpyrazolones as fluorinated analogs of antipyrine, their isomeric O-methylated derivatives resembling celecoxib structure and evaluate biological activities of obtained compounds.

Methods: *In vitro* (permeability) and *in vivo* (anti-inflammatory and analgesic activities, acute toxicity, hyperalgesia, antipyretic activity, "open field" test) experiments. To suggest the mechanism of biological activity, molecular docking of the synthesized compounds was carried out into the tyrosine site of COX-1/2.

Results: We developed the convenient methods for regioselective methylation of 1-aryl-3-polyfluoroalkylpyrazol-5-ols leading to the synthesis N-methylpyrazolones and O-methylpyrazoles as antipyrine and celecoxib analogs respectively. For the first time, the biological properties of new derivatives were investigated *in vitro* and *in vivo*.

Conclusion: The trifluoromethyl antipyrine represents a valuable starting point in design of the lead series for discovery new antipyretic analgesics with anti-inflammatory properties.

Keywords: Methylation; 1H-Pyrazol-5-ols; Polyfluoroalkyl-containing antipyrine; Analgesic and anti-inflammatory activities; Toxicity; Permeability; Molecular docking; COX-1/2 inhibitor.

1. INTRODUCTION

Formally belonging to the non-steroidal anti-inflammatory drug class, pyrazolones have long been used in medical practice. The parent compound in the series - antipyrine (AP) – was synthesized by Knorr in 1883 [1]. After its release to the market, the structure of AP was further optimized in order to improve bioavailability and efficacy as well as to diminish undesirable side effects. Therefore, aminophenazone, propyphenazone, dipyrone (a.k.a. metamizole, MET) (Fig. **1a**) and other pyrazolone scaffold based drugs (PSBDs) were obtained (see *DrugBank*). Most of them are still used by medical doctors and/or veterinarians worldwide as anti-inflammatory analgesics and antipyretics. In spite of serious limitations due to adverse drug reactions, pyrazolone drugs are comparatively safe in terms of general toxicity and gastrointestinal tract (GIT) damage. Main side effects associated with pyrazolones include individual allergic reactions and hematological disorders [2, 3]. One of the latter risks (agranulocytosis) was the reason for MET, one of the most effective non-opioid analgesics ever, withdrawal from the market in the number of countries. Later it was shown that metamizole side effects were possibly overestimated and its short-term use in the hospital setting is safer if compared with other popular analgesics [4, 5], while the risk of drug induced agranulocytosis may be managed by genetics based personalized approach to patients' treatment [6].

In the end of 1980-s, one of the AP metabolites, 3-methyl-1-phenyl-5-pyrazolone (Fig. **1b**) was approved under INN edaravone for stroke recovery treatment as a free radical acceptor [7, 8]. Over the last decade, edaravone was additionally authorized by different agencies in several countries (including FDA in 2017) for amyotrophic lateral sclerosis treatment [9].

*Address correspondence to this author at the Postovsky Institute of Organic Synthesis of the Ural Branch of the Russian Academy of Sciences, S. Kovalevskoy Str., 22, Ekaterinburg 620990, Russia; E-mail: schegolkov@ios.uran.ru

1573-4064/19 $58.00+.00

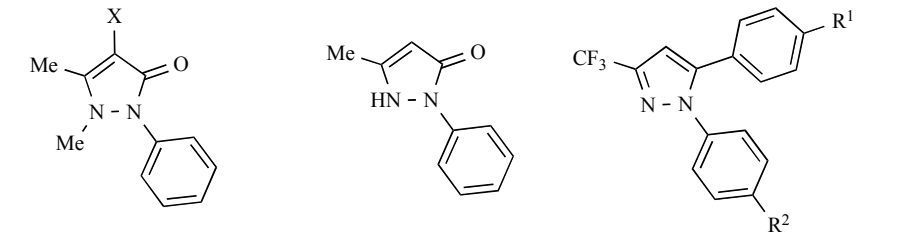

Antipyrine derivatives (a)

Antipyrine X = H

Propyphenazone X = $CH(Me)_2$

Aminophenazone X = NMe_2

Metamizole X = $N(Me)CH_2SO_3H$

Edaravone (b)

Coxib derivatives (c)

Celecoxib R^1 = Me, R^2 = SO_2NH_2

Mavacoxib R^1 = F, R^2 = SO_2NH_2

Fig. (1). AP and its derivatives (**a**), edaravone (**b**), coxib derivatives (**c**).

Pyrazolones are characterized by mild to low level of anti-inflammatory activity which contradicts their strong analgesic and antipyretic effects. Unlike other NSAIDs, they poorly inhibit COX1 / COX2 on their active sites alternatively acting *via* sequestering radicals that initiate COX catalytic activity or reducing oxidized COX protein [10]. Other mechanisms pyrazolones biological actions include, for example, the ability of MET to manifest its analgesic properties partially *via* cannabinoid system. The drug is rapidly metabolized to the products which can be further N-acylated by arachidonic acid. Formed arachidonoyl amides effectively bind to cannabinoid receptors thus producing analgesic effect [11]. Recently, it was additionally identified that analgesic action of MET and other pyrazolones is mediated by TRPA1 channel affecting the susceptibility to a variety different stimulus [12].

The multi-target nature of PSBDs seems to create a space for enhancing their anti-inflammatory activity while retaining the superior analgesic properties. The attempts to further optimize the PSBDs structures are constantly made in order to improve therapeutic outcomes in traditional NSAIDs area [13, 14] as well as to modulate different new targets [15, 16].

We expect that to achieve progress in this area fluorinated derivatives of pyrozolones should be studied, since the effectiveness of introducing fluorine to various compounds have shown to be high [17]. For example, the incorporation of fluoroalkylated substituents into the structures of organic compounds increases their solubility, lipophilicity, bioavailability, and metabolic stability [18, 19]. Besides, due to high electronegativity of fluorine atom, the fluorinated compounds are capable of forming strong intermolecular fluorine-hydrogen like nucleotide-DNA bonds [20-27]. Recently, we have shown that polyfluorinated salicylic acids and their derivatives have stronger anti-inflammatory activity than the known non-fluorinated drug aspirin [28]. Moreover, the first registered selective COX-2 inhibitors which entered the clinical and veterinarian practice are the fluorine containing pyrazoles – celecoxib (CEL) [29, 30] and mavacoxib [31] (Fig. **1c**).

Here we report the synthesis and biological activity of N-methylated 1-aryl-3-polyfluoroalkylpyrazolones as fluorinated analogs of AP and their isomeric O-methylated derivatives resembling CEL structure (Fig. **2**, compounds **2** and **3,** respectively).

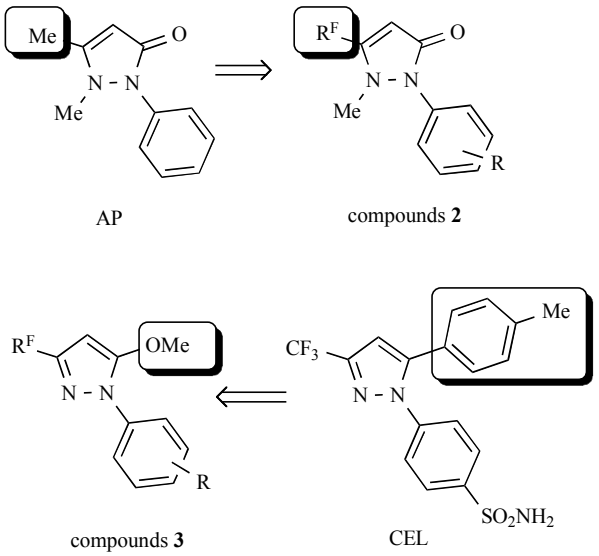

Fig. (2). Structures derived from the replacements in the molecules of AP and CEL.

2. MATERIALS AND METHOD

2.1. Chemical Part

Melting points were measured in open capillaries on "Stuart SMP30" melting point apparatus and uncorrected. The IR spectra were recorded on "Perkin Elmer Spectrum One FT-IR" by diffuse reflection accessory (DRA) and "Thermo Nicolet 6700 FT-IR" spectrometers at 4000-400 cm^{-1} using the "Frustrated total internal reflection" method (FTIR). The ^{1}H (^{13}C) NMR spectra were registered on "Bruker Avance 500" spectrometer, 500 MHz (125 MHz) relative to $SiMe_4$. The ^{19}F NMR spectra were obtained on "Bruker Avance 500" spectrometer (470 MHz) using C_6F_6 as an internal standard. The chemical shifts were converted from C_6F_6 to CCl_3F. The microanalyses (C, H, N) were carried out on "Perkin Elmer PE 2400" series II elemental analyzer. All crystal structures were solved by direct methods followed by Fourier synthesis with SHELXS-97 [32] and refined with full-matrix least-squares methods for all non-hydrogen atoms with SHELXL-97 [32] software packages. The registration of absorption was carried out analytically by the model of multi-facet crystal using a program "CrysAlisPro 1.171.29.9".

A single crystal of compound **2b** was obtained by crystallization from the diethyl ether. The X-ray studies were performed on "Xcalibur 3 CCD" diffractometer with graphite monochromator, φ\ω scanning, λMo-Kα 0.71073 Å radiation, T 295 K. Main crystallographic data for **2b**: $C_{12}H_{11}F_3N_2O$, M = 256.23, space group $P2_1/c$, monoclinic, a = 12.3613(15), b = 8.3457(9), c = 12.3094(16) Å, β = 105.077(11)°, V = 1226.2(3) $Å^3$, Z = 4, Dcalc = 1.388 $g \cdot cm^{-3}$, μ(Mo-Kα) = 0.121 mm^{-1}, 168 refinement parameters, 2990 reflections measured, 1163 unique reflections which were used in all calculations. The final R is 0.044. CCDC 1584916 contains the supplementary crystallographic data for this compound.

A single crystal of compound **3c** was obtained by crystallization from the MeOH. The X-ray studies were performed on "Xcalibur 3 CCD" diffractometer with graphite monochromator, φ\ω scanning, λCu-Kα 1.54184 Å radiation, T 295 K. Main crystallographic data for **3c**: $C_{11}H_8F_3N_3O_3$, M = 287.20, space group $P2_1/c$, monoclinic, a = 8.305(6), b = 11.807(5), c = 12.080(8) Å, β = 94.22(6)°, V = 1181.4(13) $Å^3$, Z = 4, Dcalc = 1.615 $g \cdot cm^{-3}$, μ(Cu-Kα) = 0.133 mm^{-1}, 214 refinement parameters, 2044 reflections measured, 1704 unique reflections which were used in all calculations. The final R is 0.044. CCDC 1584917 contains the supplementary crystallographic data for this compound.

2.2. Biological Part

2.2.1. Parallel Artificial Membrane Permeability Assay (PAMPA) in vitro

PAMPA was performed per the protocol for GIT test described in Instruction Manual for PAMPA Explorer (Pion, USA). Stock solutions of all compounds and standard drugs were prepared by dissolving them in 1 ml of DMSO to gain 50 mM concentration; 5 μl of each stock solution was further diluted in PBS according to the protocol and pH-map (pH=7.4, 6.2, 5.0). Firstly, the diluted solutions of all tested compounds were transferred into the UV sensitive plate (reference plate) to read the signals using Tecan Infinite M1000 PRO (Tecan, Switzerland). Secondly, donor compartment of Sandwich Stirwell Plate equipped with magnetic stirrers was column by column filled with the above mentioned diluted solutions. Lipid solution consisting of lecithin dissolved in dodecane (10% v/v), was gently dispensed on each membrane back side (5 μl per well). The Acceptor Sink Buffer (ASB) was dispensed into all wells of acceptor compartment. The acceptor plate was placed at the top of the donor plate; the whole sandwich was covered by lid and placed into Gut-Box with a wet sponge to maintain a high relative humidity thus minimizing evaporation. The assembly was allowed to incubate for 2 h and at 40 μm unstirred water layer (UWL).

After 2 h, the sandwich was removed from the Gut-Box and disassembled, both acceptor and donor compartments were separately transferred to the UV sensitive plates, and spectra were read. The results were processed with PAMPA Explorer Software.

2.2.2. In vivo Experiments

2.2.2.1. Carrageenan-induced Paw Edema Model

Anti-inflammatory activity was studied in Sprague-Dawley rats (3 male and 3 female animals per group) in the common carrageenan-induced paw edema model [33, 34]. The investigated compounds (solutions in 1% starch mucilage) were intraperitoneally (*ip*) administered at the dose of 15 mg/kg to treated group rodents 30 mins before the injection of 0.1 ml of freshly prepared 1% carrageenan (λ-carrageenan, type IV; Sigma Aldrich) solution in the right hind paw plantar surface. The negative control group consisted of rodents treated with 1% starch mucilage solution only. Diclofenac (DIF) (Hemofarm, Serbia, 10 mg/kg in 1% starch mucilage solution) or MET sodium (Moschempharm after N.A. Semashko, Russia, 15 mg/kg) were used as a reference drugs. Paw volumes were measured oncometrically with water plethysmometer (TSE Volume Meter, Germany) before carrageenan administration (at "zero time") and at 1^{st}, 3^{rd} and 5^{th} h after its injection.

To assess an anti-inflammatory activity of the sample at certain time point, first, the percentage of an edema increment (*i.e*. relative volume change for the inflamed paw vs "zero time" value) both in the negative control group (P_{neg}) and in the treated group (P_{tr}) were calculated for this time point. Then, swelling inhibition I was calculated according to the formula: 100% $(P_{neg}-P_{tr})/P_{neg}$ and considered as a measure of anti-inflammatory activity of the sample.

2.2.2.2. The Hot plate Test

The hot plate test was conducted according to established guidelines [33, 34] on Sprague-Dawley rats (3 male and 3 female rodents per group). The compounds were intraperitoneally administered in the form of suspensions in 1% starch mucilage (15 mg/kg). Negative control group animals received vehicle only (1% starch mucilage). DIF (Hemofarm, Serbia, 10 mg/kg in 1% starch mucilage solution) or MET sodium (Moschempharm after N.A. Semashko, Russia, 15 mg/kg) were used as a reference drugs. Rats were placed on an electrically heated to 50 ºC plate (Hot plate 60200 series, TSE-systems, Germany) in a plexiglas cylindrical restrainer (19 cm diameter x 30 cm). The nociceptive response time was measured by observing the appearance of rats' movements (*e.g*. jumping, hind paws licking or shaking). Maximal cutoff time was set as 30s regardless of the response. Data are expressed as a relative change of the latency time in the treated group animals compared to the corresponding value in the negative control group rats.

2.2.2.3. The Tail Flick Test

Analgesic activity was evaluated by measuring the sensitivity of Sprague-Dawley rats to heat beam applied to their tails with the Tail Flick instrument (TSE-system, Germany). To prevent tissue damage in the study the beam intensity was set to 25 % and cut-off time was limited to 60 seconds. The light beam exerting radiant heat was directed to the proximal third of the restrained animal tail. The time between tail exposure to radiant heat and escape reaction appearance was measured [33-35]. The day before the experiment was conducted, baseline testing was performed.

The rats with response time between 4 and 8 seconds were chosen and included into three groups (3 male and 3 female animals per group) for *ip* administration of one of the following: 1% starch mucilage (vehicle), **2a** (15 mg/kg in 1% starch mucilage solution) and MET sodium (Moschempharm after N.A. Semashko, Russia) (163 mg/kg in 1% starch mucilage). The latency time measurement was performed at 1st and 2nd h after compound injection [33-35].

Mean percentages of the latency time *vs* baseline were calculated for the control and treated group rodents and compared to each other statistically.

2.2.2.4. The Mechanical Hyperalgesia Test

The mechanical hyperalgesia was evaluated on Sprague-Dawley rats in Randall-Selitto test [33-36]. Three groups of animals (3 male and 3 female rodents per group) received either 1% starch mucilage (vehicle), **2a** (15 mg/kg in 1% starch mucilage solution) or reference drug DIF (Hemofarm, Serbia, 10 mg/kg) *ip* 30 mins before 0.1 ml of carrageenan solution injection. The latter was administered to the hind paw of each rat to induce inflammation. One day prior the experiment, habituation of animals to the instrument was conducted and paws of rats were manipulated with the Randall-Selitto Advanced instrument (TSE-system, Germany). The paws sensitivity was tested 1 h after carrageenan injection. The mechanical pressure was applied to the dorsal surface of the paw until the animal withdrew. At that moment maximal pressure amount (P) was recorded. The threshold was set to 530 P regardless of the response. Mean P values in treated groups were compared with one in the control group.

2.2.2.5. Evaluation of the Antipyretic Activity

Antipyretic activity was evaluated in yeast pyrexia model described in [37, 38], with slight modifications. The rectal temperatures of Sprague-Dawley rats were measured by digital thermometer (A&D, Japan). Fever was induced by subcutaneous administration of 20% (w/v) baker's yeast suspended in 0.9% saline solution (20 ml/kg) at the interscapular region. After 6 h from yeast injection, the rectal temperatures ($T_{6.0}$) were registered again and animals which showed the temperature growth not less than 1.0 °C were used for further experiment. Three group of rats (3 male and 3 female animals per group) were intraperitoneally administrated either **2a** (30 mg/kg in 1% starch mucilage solution) or Paracetamol ("Medisorb", Russia, 100 mg/kg 1% in starch mucilage solution) or 1% starch mucilage solution as vehicle control. Rectal temperatures for all rats were measured at 7th, 7.5 and 8.5 h after yeast injection.

Relative rectal temperature changes for each group at each time point were calculated: $\Delta T_{rect} = (T_{ex} - T_{6.0})/T_{6.0} \cdot 100\%$, where T_{ex}– rectal temperature at the corresponding time point of the experiment, $T_{6.0}$–temperature at 6th h after yeast administration.

2.2.2.6. Open Field Test

The open field test was conducted for evaluating exploratory, anxiety-related behavior and general activity of CD-1 mice [33, 39, 40]. Two groups of animals (5 male and 5 female mice per group) were *ip* administrated with either **2a** (suspension in 1% starch mucilage, 15 mg/kg) or the vehicle (1% starch mucilage solution). 1 h after injection, mice were one by one placed in the center of a white circular arena (diameter 63 cm, OOO Open Science, Russia) and their movements were recorded for 5 min with digital camera. The following behavioral patterns were analyzed: line crossing (in two peripheral sectors), central square entries, rearing (with and without support), grooming, defecation, urination, number and duration of fading and holes inspection. Numbers of patterns and duration of actions in the treated and control groups were analyzed statistically.

2.2.2.7. Acute Toxicity Evaluation

OECD recommendations [41] and guidelines for preclinical study of medicinal products [34] were used to set acute toxicity evaluation. Three CD-1 mice per one dose were applied. The tested compounds in 1% starch mucilage solution were injected *ip*. Animals were observed during 14 days, the number of deaths was counted.

2.2.3. Statistical Analysis

The data were analyzed by a statistical software package GraphPad Prism 6 using the «Multiplet tests» approach. The values were considered significantly different at $p < 0.05$.

3. EXPERIMENTAL

3.1. Synthesis of Pyrazolols

Pyrazololes **1a-g** have been obtained from the corresponding 4-polyfluoroalkyl-3-oxo esters with substituted hydrazines by the known method [42].

3.1.1. 1-Phenyl-3-trifluoromethyl-1H-pyrazol-3-ol (1a)

Yield 81%, off-white powder, mp 193–194 °C (lit. [43], mp 191–192 °C).

3.1.2. 1-(4-Methylphenyl)-3-trifluoromethyl-1H-pyrazol-5-ol (1b)

Yield 60%, colorless crystals, mp 218-219 °C. ^{1}H NMR (DMSO-d_6): δ 2.35 (s, 3H, Me), 5.91 (s, 1H, CH), 7.31, 7.57 (both d, 4H, C_6H_4, *J* 8.3 Hz), 12.33 (s, 1H, OH). ^{19}F NMR (DMSO-d_6): δ -62.0 (s, CF_3).

3.1.3. 1-(4-Nitrophenyl)-3-trifluoromethyl-1H-pyrazol-5-ol (1c)

Yield 65%, orange crystals, mp 125 °C subl. ^{1}H NMR (DMSO-d_6): δ 5.99 (s, 1H, CH), 8.11, 8.38 (both d, 4H, C_6H_4, *J* 9.2 Hz), OH is not observed. ^{19}F NMR (DMSO-d_6): δ -62.6 (s, CF_3).

3.1.4. 1-(3-Chlorophenyl)-3-trifluoromethyl-1H-pyrazol-5-ol (1d)

Yield 85%, colorless crystals, mp 210-211 °C. ^{1}H NMR (DMSO-d_6): δ 5.96 (s, 1H, CH), 7.46, 7.55, 7.75, 7.80 (all m, 4H, C_6H_4), 12.77 (s, 1H, OH). ^{19}F NMR (DMSO-d_6): δ -62.3 (s, CF_3).

3.1.5. 3-Trifluoromethyl-1-(3-trifluoromethylphenyl)-1H-pyrazol-5-ol (1e)

Yield 73%, colorless crystals, mp 204-205 °C. ^{1}H NMR (DMSO-d_6): δ 5.99 (s, 1H, CH), 7.77, 8.12 (both m, 4H,

C_6H_4), 12.89 (s, 1H, OH). ^{19}F NMR (DMSO-d_6): δ -62.4 (s, 3F, CF_3), -61.6 (s, 3F, C_{Ar}–CF_3).

3.1.6. 1-Benzyl-3-trifluoromethyl-1H-pyrazol-5-ol (1f)

Yield 65%, white powder, mp 223-224 °C (lit. [44], mp 224.5-225.5 °C).

3.1.7. 3-Pentafluoroethyl-1-phenyl-1H-pyrazol-3-ol (1g)

Yield 70%, off-white powder, mp 210-211°C (lit. [45] in Supplementary, mp 209-210°C).

3.2. Typical Procedure for N-methylation of pyrazoles 1a–g

A 3.15 g, 25 mmol of dimethyl sulfate was added to 5 mmol of pyrazoles **1a-g**. The flask was immersed in the oil bath and heated at 120-130 °C for 6-7 h. After cooling, 30 ml of ether was added and the resulting precipitate was isolated and washed by 10% sodium hydroxide. The residue was purified by column chromatography (eluent – $CHCl_3$).

3.2.1. 1-Methyl-2-phenyl-5-trifluoromethyl-1,2-dihydro-3H-pyrazol-3-one (2a)

Yield 77%, colorless crystals, mp 138-139 °C (lit. [46], mp 138-139 °C).

3.2.2. 1-Methyl-2-(4-methylphenyl)-5-trifluoromethyl-1,2-dihydro-3H-pyrazol-3-one (2b)

Yield 58%, colorless crystals, mp 122-123°C. IR (DRA): ν 1660 (C=O), 1613, 1584, 1515 (C=C), 1257-1171 (C–F) cm^{-1}. ^{1}H NMR (DMSO-d_6): δ 2.37 (s, 3H, *p*-Me), 3.18 (s, 3H, Me), 6.25 (s, 1H, CH), 7.29, 7.36 (both d, 4H, C_6H_4, *J* 8.3 Hz). ^{13}C NMR (DMSO-d_6): δ 20.61 (s, *p*-Me), 36.33 (s, Me), 100.42 (q, CH, *J* 2.6 Hz), 119.11 (q, CF_3, *J* 271.0 Hz), 125.72, 129.81, 130.23, 137.86 (C_6H_4), 143.09 (q, *C*—CF_3, *J* 38.5 Hz), 162.02 (C=O). ^{19}F NMR (DMSO-d_6): δ -62.2 (s, CF_3). Anal. calcd. for $C_{12}H_{11}F_3N_2O$. C, 56.25; H, 4.33; N, 10.93. Found: C, 56.24; H, 4.16, N, 10.86.

3.2.3. 2-(4-Nitrophenyl)-1-methyl-5-trifluoromethyl-1,2-dihydro-3H-pyrazol-3-one (2c)

Yield 68%, yellow crystals, mp 133-136°C. IR (DRA): ν 1695 (C=O), 1591, 1521, 1493 (C=C), 1171, 1143 (C–F) cm^{-1}. ^{1}H NMR ($CDCl_3$): δ 3.25 (s, 3H, Me), 6.13 (s, 1H, CH), 7.65, 8.39 (both d, 4H, C_6H_4, *J* 9.0 Hz). ^{13}C NMR ($CDCl_3$): δ 38.03 (q, Me, *J* 1.2 Hz), 103.88 (q, CH, *J* 2.7 Hz), 118.90 (q, CF_3, *J* 271.6 Hz), 123.48, 125.02, 138.83, 145.87 (C_6H_4), 148.72 (q, *C*—CF_3, *J* 39.1 Hz), 163.37 (C=O). ^{19}F NMR ($CDCl_3$): δ -64.4 (s, CF_3). Anal. calcd. for $C_{11}H_8F_3N_3O_3$. C, 46.00; H, 2.81; N, 14.63. Found: C, 46.08; H, 2.85, N, 14.44.

3.2.4. 2-(3-Chlorophenyl)-1-methyl-5-trifluoromethyl-1,2-dihydro-3H-pyrazol-3-one hemihydrate (2d)

Yield 57%, light-yellow crystals, mp 85-87°C. IR (DRA): ν 1681 (C=O), 1661, 1587, 1480 (C=C), 1259-1177 (C–F) cm^{-1}. ^{1}H NMR (DMSO-d_6): δ 3.21 (s, 3H, Me), 6.35 (s, 1H, CH), 7.38-7.41, 7.50-7.61 (all m, 4H, C_6H_4). ^{13}C NMR (DMSO-d_6): δ 36.91 (q, Me, *J* 1.3 Hz), 101.18 (q, CH, *J* 2.8 Hz), 119.02 (q, CF_3, *J* 271.2 Hz), 123.59, 124.82, 127.75, 130.98, 133.53, 134.19 (C_6H_4), 144.70 (q, *C*—CF_3, *J* 38.5 Hz), 162.29 (C=O). ^{19}F NMR (DMSO-d_6): δ -62.3 (s, CF_3). Anal. calcd. for $C_{11}H_9F_3ClN_2O_{1.5}$. C, 46.25; H, 3.18; N, 9.81. Found: C, 46.26; H, 2.95, N, 9.60.

3.2.5. 1-Methyl-5-trifluoromethyl-2-(3-trifluoromethylphenyl)-1,2-dihydro-3H-pyrazol-3-one (2e)

Yield 60%, light-yellow crystals, mp 56-58 °C. IR (DRA): ν 1672 (C=O), 1610, 1587, 1492, 1446 (C=C), 1268-1172 (C–F) cm^{-1}. ^{1}H NMR ($CDCl_3$): δ 3.23 (s, 3H, Me), 6.10 (s, 1H, CH), 5.15 (s, 2H, CH_2), 7.64-7.67 (m, 4H, C_6H_4). ^{13}C NMR ($CDCl_3$): δ 37.33 (q, Me, *J* 1.2 Hz), 102.82 (q, CH, *J* 2.8 Hz), 119.00 (q, CF_3, *J* 271.4 Hz), 123.45 (q, CF_3, *J* 272.6 Hz), 121.26 (q, C_o, *J* 3.8 Hz), 124.57 (q, C_p, *J* 3.5 Hz), 132.20 (q, C_m, *J* 33.2 Hz), 127.89, 130.25, 133.84 ($C_{o'}$, $C_{p'}$, C_i), 147.00 (q, *C*—CF_3, *J* 39.1 Hz), 163.35 (C=O). ^{19}F NMR ($CDCl_3$): δ -64.3 (s, 3F, CF_3), -63.8 (s, 3F, C_{Ar}-CF_3). Anal. calcd. for $C_{12}H_8F_6N_2O$. C, 46.46; H, 2.60; N, 9.03. Found: C, 46.51; H, 2.69, N, 8.93.

3.2.6. 2-Benzyl-1-methyl-5-trifluoromethyl-1,2-dihydro-3H-pyrazol-3-one (2f)

Yield 50%, crystallizing oil, IR (FTIR): ν 1676 (C=O), 1606, 1576, 1498 (C=C), 1260-1142 (C–F) cm^{-1}. ^{1}H NMR ($CDCl_3$): δ 3.36 (s, 3H, Me), 5.15 (s, 2H, CH_2), 6.02 (s, 1H, CH), 7.20-7.21, 7.32-7.37 (both m, 5H, Ph). ^{13}C NMR ($CDCl_3$): δ 35.00 (q, Me, *J* 1.5 Hz), 45.46 (CH_2), 98.41 (q, CH, *J* 2.6 Hz), 118.85 (q, CF_3, *J* 270.9 Hz), 126.90, 128.26, 129.05, 134.90 (Ph), 141.19 (q, *C*—CF_3, *J* 39.1 Hz), 163.04 (C=O). ^{19}F NMR ($CDCl_3$): δ -63.9 (s, CF_3). Anal. calcd. for $C_{12}H_{11}F_3N_2O$. C, 56.25; H, 4.33; N, 10.93. Found: C, 56.34; H, 4.37, N, 10.85.

3.2.7. 1-Methyl-5-pentafluoroethyl-2-phenyl-1,2-dihydro-3H-pyrazol-3-one (2g)

Yield 71%, orange crystals, mp 82-83 °C (lit. [46], mp 82-83 °C).

3.3. Typical Procedure for O-methylation of Pyrazoles 1a–g

A mixture of 5 mmol of pyrazoles **1a-g**, 0.63 g, 5 mmol of dimethyl sulfate and 1.04 g, 7.5 mmol of K_2CO_3 in 10 ml of acetonitrile was refluxed for 6-7 h. After cooling, 30 ml of water was added and the solution was extracted with 2x30ml ether. The ether was removed and the residue was purified by appropriate method.

3.3.1. 5-Methoxy-1-phenyl-3-trifluoromethyl-1H-pyrazole (3a)

Yield 73%, yellow oil [46].

3.3.2. 5-Methoxy-1-(4-methylphenyl)-3-trifluoromethyl-1H-pyrazole (3b)

Yield 80%, yellow oil. IR (FTIR): ν 1593, 1568, 1521, 1497 (C=C, C=N), 1250-1155 (C-F) cm^{-1}. ^{1}H NMR ($CDCl_3$): δ 2.38 (s, 3H, *p*-Me), 3.96 (s, 3H, Me), 5.93 (s, 1H, CH), 7.24, 7.53 (both d, 4H, C_6H_4, *J* 8.4 Hz). ^{13}C NMR ($CDCl_3$): δ 21.02 (*p*-Me), 59.18 (Me), 83.97 (q, CH, *J* 2.0 Hz), 121.06 (q, CF_3, *J* 268.9 Hz), 122.84, 129.50, 135.19, 137.55 (C_6H_4), 141.53 (q, *C*—CF_3, *J* 38.5 Hz), 155.51 (*C*–OMe). ^{19}F NMR ($CDCl_3$): δ -64.4 (s, CF_3). Anal. calcd. for $C_{12}H_{11}F_3N_2O$. C, 56.25; H, 4.33; N, 10.93. Found: C, 56.22; H, 4.18, N, 11.15.

3.3.3. 5-Methoxy-1-(4-nitrophenyl)-3-trifluoromethyl-1H-pyrazole (3c)

Yield 75%, yellow crystals, mp 111-112 °C. IR (FTIR): ν 1611, 1598, 1580, 1519, 1495 (C=C, C=N), 1224-1155 (C-F) cm^{-1}. ^1H NMR ($CDCl_3$): δ 4.08 (s, 3H, Me), 6.00 (s, 1H, CH), 8.02, 8.32 (both m, 4H, C_6H_4). ^{13}C NMR ($CDCl_3$): δ 59.74 (Me), 85.00 (q, CH, *J* 1.6 Hz), 120.60 (q, CF_3, *J* 269.4 Hz), 121.80, 124.64, 142.75, 145.86 (C_6H_4), 143.30 (q, *C*—CF_3, *J* 38.9 Hz), 156.52 (*C*–OMe). ^{19}F NMR ($CDCl_3$): δ -64.9 (s, CF_3). Anal. calcd. for $C_{11}H_8F_3N_3O_3$. C, 46.00; H, 2.81; N, 14.63. Found: C, 46.10; H, 2.84, N, 14.49.

3.3.4. 1-(3-Chlorophenyl)-5-methoxy-3-trifluoromethyl-1H-pyrazole (3d)

Yield 62%, orange crystals, mp 47-49 °C. IR (DRA): ν 1589, 1568, 1496, 1477 (C=C, C=N), 1246-1119 (C-F) cm^{-1}. ^1H NMR (DMSO-d_6): δ 4.03 (s, 3H, Me), 6.51 (s, 1H, CH), 7.51, 7.57, 7.68, 7.75 (all m, 4H, C_6H_4). ^{13}C NMR (DMSO-d_6): δ 60.13 (Me), 85.48 (q, CH, *J* 1.7 Hz), 120.99 (q, CF_3, *J* 268.8 Hz), 120.99, 122.06, 127.58, 130.98, 133.46, 138.26 (C_6H_4), 140.95 (q, *C*—CF_3, *J* 37.8 Hz), 156.09 (*C*–OMe). ^{19}F NMR (DMSO-d_6): δ -62.3 (s, CF_3). Anal. calcd. for $C_{11}H_8F_3ClN_2O$. C, 47.76; H, 2.91; N, 10.13. Found: C, 47.53; H, 2.89, N, 9.98.

3.3.5. 5-Methoxy-3-trifluoromethyl-1-(3-trifluoromethyl-phenyl)-1H-pyrazole (3e)

Yield 70%, colorless crystals, mp 43-45 °C. IR (FTIR): ν 1601, 1575, 1509, 1464 (C=C, C=N), 1256-1150 (C—F) cm^{-1}. ^1H NMR ($CDCl_3$): δ 4.02 (s. 3H, Me), 5.97 (s, 1H, CH), 7.59, 7.93, 8.02 (all m, 4H, C_6H_4). ^{13}C NMR ($CDCl_3$): δ 59.50 (Me), 84.50 (CH), 120.82 (q, CF_3, *J* 269.2 Hz), 123.61 (q, C_{Ar}—*C*F_3, *J* 272.5 Hz), 119.27 (q, C_o, *J* 3.8 Hz), 123.29 (q, C_p, *J* 3.6 Hz), 125.44, 129.63, 138.23 ($C_{o'}$, $C_{p'}$, C_i), 131.59 (q, C_m, *J* 33.1 Hz), 142.52 (q, *C*—CF_3, *J* 38.9 Hz), 155.96 (*C*–OMe). ^{19}F NMR ($CDCl_3$): δ -64.6 (s, 3F, CF_3), -63.8 (s, 3F, C_{Ar}—CF_3). Anal. calcd. for $C_{12}H_8F_6N_2O$. C, 46.16; H, 2.60; N, 9.03. Found: C, 45.98; H, 2.61, N, 8.80.

3.3.6. 1-Benzyl-5-methoxy-3-(trifluoromethyl)-1H-pyrazole (3f)

Yield 55%, yellow oil. IR (FTIR): ν 1606, 1571, 1499, 1456, 1431 (C=C, C=N), 1134-1245 (C—F) cm^{-1}. ^1H NMR ($CDCl_3$): δ 3.81 (s, 3H, Me), 5.10 (s, 2H, CH_2), 5.73 (s, 1H, CH), 7.15, 7.24 (both m, 5H, Ph). ^{13}C NMR ($CDCl_3$): δ 51.27 (Me), 59.02 (CH_2), 83.22 (q, CH, *J* 1.7 Hz), 121.08 (q, CF_3, *J* 268.7 Hz), 121.52, 127.87, 128.65, 135.86 (Ph), 140.64 (q, *C*—CF_3, *J* 38.3 Hz), 155.44 (*C*—OMe). ^{19}F NMR ($CDCl_3$): δ -64.1 (s, CF_3). Anal. calcd. for $C_{12}H_{11}F_3N_2O$. C, 56.25; H, 4.33; N, 10.93. Found: C, 56.30; H, 4.25, N, 10.70.

3.3.7. 5-Methoxy-3-pentafluoroethyl-1-phenyl-1H-pyrazole (3g)

Yield 75%, yellow oil. IR (FTIR): ν 1597, 1569, 1510, 1484 (C=C, C=N), 1214-1137 (C–F) cm^{-1}. ^1H NMR ($CDCl_3$): δ 3.97 (s, 3H, Me), 5.95 (s, 1H, CH), 7.31-7.35, 7.42-7.46, 7.67-7.69 (all m, 5H, Ph). ^{13}C NMR ($CDCl_3$): δ 59.24 (Me), 85.23 (CH), 110.59 (tq, CF_2, *J* 251.0, 39.1 Hz), 118.85 (qt, CF_3, *J* 286.0, 38.0 Hz), 122.80, 127.54, 128.96, 137.70 (Ph), 140.39 (t, *C*—C_2F_5, *J* 28.7 Hz), 155.82 (*C*—OMe). ^{19}F NMR ($CDCl_3$): δ -115.1 (q, 2F, CF_2, *J* 2.5 Hz), -85.4 (t, 3F, CF_3, *J* 2.5 Hz). Anal. calcd. for $C_{12}H_9F_5N_2O$. C, 49.32; H, 3.10; N, 9.59. Found: C, 49.10; H, 2.98, N, 9.52.

4. RESULTS AND DISCUSSIONS

4.1. Chemistry

The synthesis of trifluoromethyl-substituted AP **2a** was described in 1958 without proof of its structure [47]. Later, its analog containing the second trifluoromethyl-group in phenyl substituent was obtained [48], but it also had been not characterized. However, the methylation of 1-aryl-3-polyfluoroalkyl-1*H*-pyrazol-5-ols **1** may lead to formation of isomeric O-methylated products.

Recently we developed [46] the convenient approaches to selective O- and N-methylation of 1-aryl-3-polyfluoroalkyl-1*H*-pyrazol-5-ols **1**. The best conditions for chemoselective N-methylpyrazolones **2** synthesis were found to be a heating of pyrazolols **1a-g** with 5 equiv of dimethyl sulphate while O-methylpyrazoles **3** can be obtained as the only products by refluxing of compounds **1a-g** with **1** equiv of dimethyl sulphate and 1.5 equiv of K_2CO_3. Herein, using these procedures, we synthesized a series of NMe-substituted pyrazolones **2a-g** and OMe-containing pyrazoles **3a-g** (Scheme **1**) with the various polyfluoroalkyl and aryl substituents.

A chemical shift of methyl group at the heteroatom is a convenient criterion for distinction of isomers **2** and **3**. Thus, the ^1H NMR spectra of compounds **2a-g** contain the signals of NMe fragment at δ 3.2…3.3 ppm, while the signals of OMe group are observed at δ 3.8…4.1 ppm in pyrazoles **3a-g**. Moreover, the IR spectra of N-isomers **2a-g** have a high-frequency absorption band of carbonyl group at 1695-1660 cm^{-1} in contrast to O-methylated products **3a-g**.

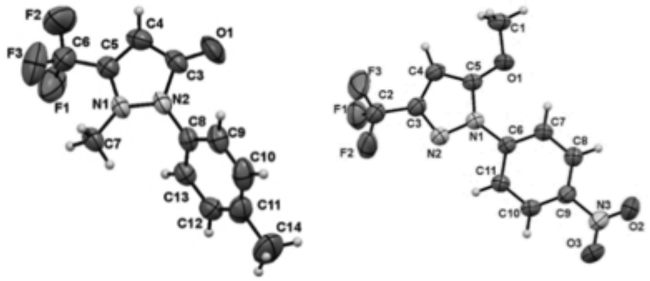

Fig. (3). The ORTEP view of molecules **2b** and **3c**.

We managed to grow up the monocrystals for both isomers and carried out the X-Ray analysis of NMe pyrazolone **2b** (Fig. **3**, CCDC 1584916) and OMe pyrazole **3c** (Fig. **3**, CCDC 1584917). This clearly confirmed the regioisosteric structure of pyrazoles **2** and **3**.

The development of convenient methods for pyrazoles **2** and **3** synthesis allowed us to study their biological properties as potential NSAIDs.

4.2. Biological Evaluation

The goal of our study was to obtain the fluorinated AP derivatives which a) have enhance analgesic potency, b) elicit anti-inflammatory effect and c) are less toxic or have

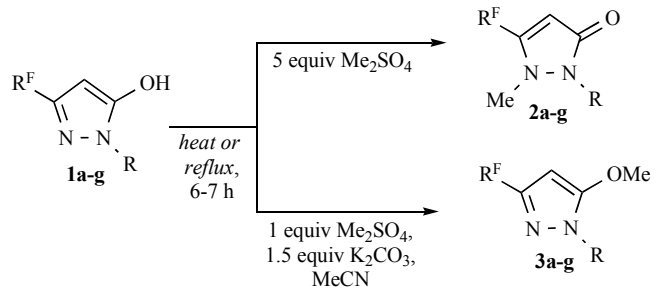

$R^F = CF_3$, R = Ph (**a**), C_6H_4Me-4 (**b**), $C_6H_4NO_2$-4 (**c**), C_6H_4Cl-3 (**d**), $C_6H_4CF_3$-3 (**e**); CH_2Ph (**f**),
$R^F = C_2F_5$, R = Ph (**g**).

Scheme 1. Synthesis of N- and O-methylated pyrazoles.

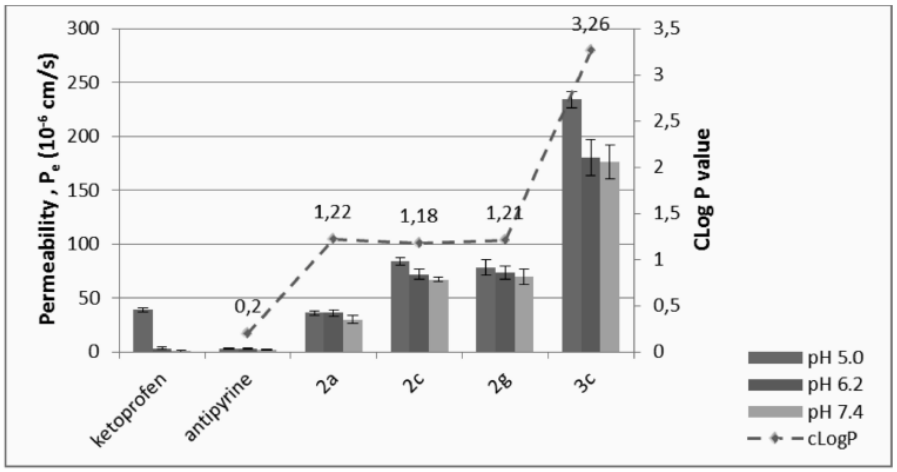

Fig. (4). Permeability P_e (10^{-6} cm/s) – lipophilicity (ClogP) relationship for AP and its derivatives.

favorable pharmacokinetics which would allow lowering the therapeutic doses and, hence, diminishing the undesirable side effects. Several factors, such as the "multi-targetness" of pyrazolone scaffold, diverse profiles of biological action for non-fluorinated AP derivatives and different patterns of metabolic activation of the PSBDs [49, 50] may imply that the biological evaluation *in vivo* could be more informative for the lead series elucidation. One of the most beneficial methods to identify a multi-target lead compound as well as any relevant pro-drugs is phenotypic screening since all the involved targets and the metabolic activation factors can be engaged at ones in the *in vivo* experiment.

For the sake of this research, we have chosen the mixed strategy which includes preliminary evaluation of the limited set of derivatives in simple models of pain and inflammation (hot plate test and carrageenan-induced edema test respectively). The test involving carrageenan was supposed to be performed for only those compounds which were active in the hot plate test since analgesic activity evaluations were considered as a primary goal.

4.2.1. ADME Analysis

To determine the possibility of synthesized compounds theoretical hitting into «drug like space» ADME analysis was performed [51, 52]. The compounds bioavailability was assessed with Maestro Elements 2.4 (QikProp) program [53]. The calculation results are presented in Table **1**. The compounds **2a-g**, **3a-g** fall into the Lipinski rule of five because their molecular weights are not higher 500 Da, the predicted values of lipophilicity (AlopP) do not exceed 5, the quantity of hydrogen bonds (donor or acceptor) is no more than 2, rotating bonds are no more than 4, and at last, the calculated polar surface areas of the structures are no more than 70 Å. This means that the synthesized compounds comply the "rules of thumb" applied in drug discovery, including the Lipinski's rule of five [54] and for compounds **1a, 2a,f** even more strict criteria - the "rule of three" [55].

4.2.2. Permeability Study in vitro

Further, in *in vitro* experiment we evaluated the impact of fluorine atoms on the AP derivatives permeability. The ability of AP and synthesized compounds **2a,c,g** and **3a,c** to passively diffuse through the membranes was assessed in Parallel Artificial Membrane Permeability Assay (PAMPA) [56, 57] at pH values simulating the media in different parts of the GIT (5.0, 6.2 and 7.4). Ketoprofen was used as a reference drug with high permeability at acidic pH. Additionally, lipophilicity, represented as ClogPs, was calculated in ChemBioDraw Ultra® 13.0.2.302. The lipophilicity–permeability relationship of the tested compounds is presented in the diagram below (Fig. **4**).

The figure shows that the compounds **2a,c,g** and **3c** penetrate through an artificial membrane much better than AP at all pH values. Thus, substitution of methyl group to

Table 1. ADME parameters.

ID Ligand	Molecular Weight, Da	Hydrogen Bond		Lipophilicity (AlogP)	Polar Surface Area, Å^2	Rotatable Bond	QPlogP$_{o/w}$[c]	QPlogKp[d]	Human Oral Absorption[e]
		Donor	Acceptor						
Constrains	500.0[a]	5	10	5.00	140.00	10	-2.0 – 6.5	-8.0 – -1.0	> 80 is high < 25% is poor
	300.0[b]	3	3	3.00	60.00	3			
DIF	296.15	1	0	3.67	56.16	4	4.50	-1.87	100.0
CEL	327.90	2	3	4.06	86.41	5	3.36	-3.20	92.4
SC560	352.75	0	2	5.55	27.05	4	5.98	-0.64	100.0
1a	227.20	0	1	2.55	40.88	2	3.44	-1.57	100.0
2a	242.20	0	1	2.86	26.93	2	2.17	-1.69	100.0
2b	256.23	0	1	3.35	26.93	2	2.56	-1.89	100.0
2c	287.20	0	1	2.75	70.07	3	1.65	-3.60	82.9
2d	276.65	0	1	3.52	26.93	2	2.92	-1.86	100.0
2e	310.20	0	1	3.80	26.93	3	3.37	-1.91	100.0
2f	256.23	0	1	2.87	26.93	3	2.78	-1.51	100.0
2g	292.20	0	1	3.35	26.90	3	3.09	-1.63	100.0
3a	242.20	0	2	3.48	27.05	3	4.33	-0.81	100.0
3b	256.23	0	2	3.97	27.05	3	4.65	-1.01	100.0
3c	287.20	0	2	3.38	70.19	4	3.36	-2.72	100.0
3d	276.65	0	2	4.15	27.05	3	4.83	-0.98	100.0
3e	310.20	0	2	4.42	27.05	4	5.34	-1.04	100.0
3f	256.23	0	2	3.49	27.05	4	4.70	-0.65	100.0
3g	292.21	0	2	3.97	27.05	4	5.00	-0.75	100.0

[a] rules of five; [b] rules of three; [c] predict octanol/water partition coefficient; [d] predict skin permeability, log K_p; [e] predict human oral adsorption;

CF_3 group in pyrazolone ring of AP (compound **2a**) on average allowed 15 times permeability increase. More impressive difference is observed when the data for O-methylated pyrazole **3c** is compared with one for corresponding N-derivative (compound **2c**). Unexpectedly, for derivative **3a** we observed low signals in both donor and acceptor compartments far below the level in the reference solution. Since **3a** is fairly stable in the assay conditions, its localization in the lipid membrane may serve as a putative explanation for its disappearance from the compartments. Moreover, the **3a** lipophilicity is the highest among all compounds tested in PAMPA. While high lipophilicity can lead to GIT absorption complication, it may be favorable for the tissue distribution of the compound [58]. Overall, the PAPMA data demonstrates that fluorinated derivatives possibly have an advantage in terms of bioavailability and pharmacokinetic properties compared with AP.

4.2.3. Acute Toxicity Study

In order to briefly estimate the toxicity of the synthesized compounds and to choose an appropriate dose for their *in vivo* efficacy evaluation, the compounds were assessed first in the acute toxicity test in CD-1 mice (3 rodents per dose). The obtained data (Table **2**) allows us to conclude that LD_{50} values for the most of the synthesized fluorinated AP derivatives are expected to be significantly over 150 mg/kg (*ip*), *e.g.* all compounds are substantially less toxic than DIF [59]. Compounds **1a**, **2a**,**b, g** seem to be more toxic than AP and MET (see Table **2**).

When compared the data for **2a** vs **3a**, **2b** vs **3b** may imply that O-methylated derivatives **3** are slightly less toxic than the corresponding N-methylated derivatives **2.** Both isomeric pyrazoles **2e** and **3e,** having *meta*-CF_3-group in aryl substituent, are not toxic at the dose of 300 mg/kg. Two routes of administration (*ip* and *per os*) were tested for the **2a** compound and application of the latter leads to significantly lower level of acute toxicity (expected LD_{50} > 600 mg/kg).

Based on the toxicity data and the perspective to easily elucidate the most promising compounds due to rather strict threshold, the dose of 15 mg/kg was chosen for synthesized compounds biological activity evaluation. In order to avoid

Table 2. Anti-inflammatory, analgesic activity and acute toxicity of fluorinated pyrazoles *in vivo*.

Compound	Dose, mg/kg	Anti-inflammatory Activity, Swelling Inhibition, %			Analgesic Activity, Latent Period Prolongation,%	Acute Toxicity [a]
		After 1 h	After 3 h	After 5 h		
1a	15	n/t	n/t	n/t	54.5 **	300 (2)
2a	15	56.8 *	51.1 ***	29.0 *	128.0 ***	150 (0) 225 (0)
	10	n/a	25.69 *	n/a	59.3 ***	300 (2) 300 [b] (0) 600 [b] (0)
2b	15	n/a	n/a	n/a	82.6 ***	150 (0) 300 (1)
2c	15	n/a	-32.52 *	n/a	20.5 §	150 (0)
2d	15	n/a	n/a	n/a	n/a	150 (0)
2e	15	n/a	n/a	n/a	n/a §§	150 (0) 300 (0)
2g	15	n/a §§§	n/a	n/a	51.1 ****	150 (0) 300 (1)
3a	15	n/a	n/a	n/a	82.9 **	150(0) 300 (0)
	0	n/t	n/t	n/t	53.3*, 82.4[c]***	600 (0)
3b	15	n/t	n/t	n/t	60.2 ***	300 (0)
3c	15	n/t	n/t	n/t	n/a n/a[c]	150 (0)
3e	15	n/t	n/t	n/t	n/a	150 (0) 300 (0)
MET	15	n/a[d]	n/a[d]	n/a[d]	59.8 - 93.8[e]	LD_{50} 2160-3340, mice, *ip* [61]
DIF	10	53.9 ± 7.1[f]	61.8 ± 10.8[f]	48.5 ± 13.1[f]	44.0 – 70.9[g]	LD_{50} 74, mice, *ip* [59]

n/a – not active; n/t – not tested; [a] represented as a dose, mg/kg (number of mice which did not survive of the three ones taken in the experiment); [b] tested at *per os* route; [c] measured 120 min after sample administration; [d] data from two independent experiments; [e] interval of values obtained in five different independent experiments; [f] median for five different independent experiments ± standard deviation; [g] interval of values obtained in four different independent experiments; § trend is observed**:** p=0.05**;** §§ trend is observed**:** 36.3%, p=0.08;§§§ trend is observed**:** 30.4%, p=0.07;* p<0.05; ** p<0.01; ***p<0.001; ****p<0.0001

compounds degradation in the GIT, the samples were administered intraperitoneally.

4.2.4. Analgesic Activity Study

Some of the synthesized compounds were first assessed for analgesic activity in the hot plate test in rats [33] at the dose of 15 mg/kg (Table **2**). Since AP high doses are required for achieving an anti-nociceptive response in the hot plate test [34, 62], more effective pyrazolone analgesic MET was chosen as a reference drug.

The CF_3-AP **2a** elicits the most prominent anti-nociceptive effect exceeding such of MET at the same dose (15 mg/kg). The lower dose of **2a** (10 mg/kg) produces approximately two-times weaker analgesic effect. Being administered at the dose of 15 mg/kg the N-methylated derivatives **2a, b** are more potent than the corresponding O-methylated isomers **3a,b**, although compound **3a** exhibits a fairly strong analgesic effect (82.9 % latency time prolongation). Interestingly, the **3a** dose decrease to 10 mg/kg leads to notably weaker effect (53.3%) at the 1st h after the injection, however, at the 2nd h the activity restores to 82.4%

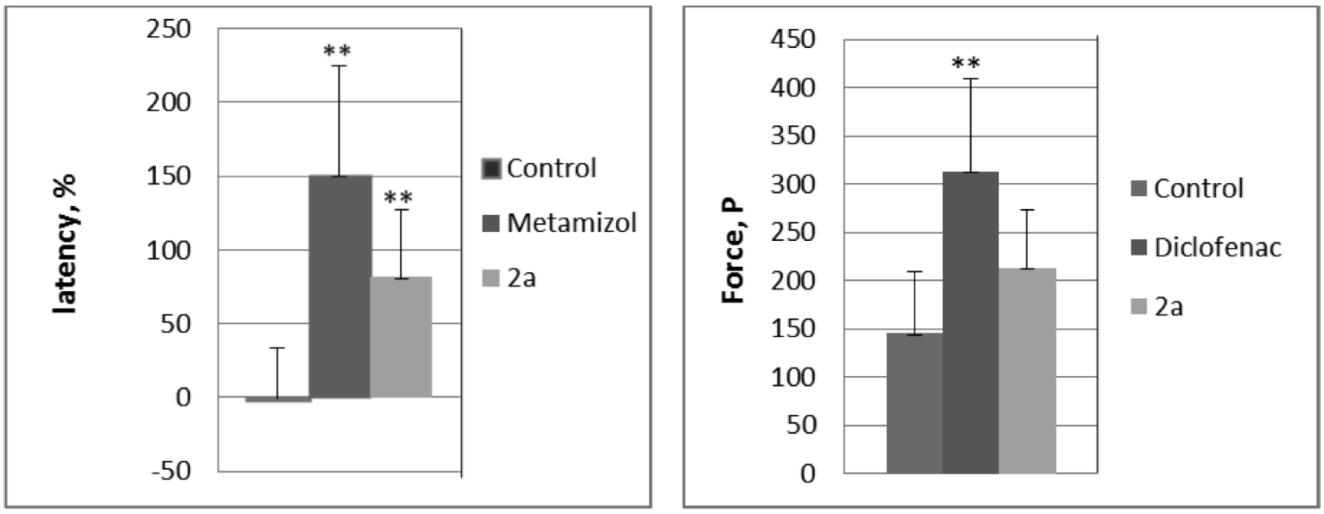

A **B**

Fig. (5). Analgesic activity of **2a,** represented as mean values±SD: **A**. in the "tail flick" test (**2a** at 15 mg/kg, n=6; MET at 163 mg/kg, n=5); **B**. in the Randall-Selitto test of carrageenan-induced hyperalgesia in rats (**2a** at 15 mg/kg, n=6; DIF at 10 mg/kg, n=6). **p<0.01 compared to the vehicle treated control.

latency time. Such data may imply the compounds pharmacokinetics profile further investigation importance or metabolic activation occurrence. The parent pyrazole **1a**, which was tested for the structure-activity analysis, demon-strated evident analgesic activity: a dose of 15 mg/kg caused the latent period prolongation by 54.5%.

The structure-activity analysis showed that polyfluoroalkyl substituent elongation causes partial loss of analgesic activity (C_2F_5-AP **2g** *vs* CF_3-AP **2a**). Additionally, substituent in aryl fragment of pyrazoles **2** and **3** negatively influences their anti-nociceptive properties. Thus, compounds **2a**, **3a,** having unsubstituted phenyl moiety, are the most potent. Electron-withdrawing substituents in both *para*- and *meta*-positions of aryl fragment abolish the activity for all tested compounds (**2c**, **2d** and **2e** *vs* **2a**; **3c** and **3d** *vs* **3a**). The presence of an electron-donating methyl group substantially reduces the activity (**2b** *vs* **2a**; **3b** *vs* **3a**).

Overall, the correlation between anti-nociceptive properties and permeability/ lipophilicity is absent for the synthesized compounds: all of them (both active and not active) are more lipophilic than AP. This may imply that the membrane permeability is not the limiting factor for exhibiting analgesic activity by synthesized pyrazolone derivatives.

PSBDs are quite rapid and extensively metabolized *in vivo* and most of their biological effects are often ascribed to their metabolites [11-13, 48-49]. The obtained patterns of the structure-activity relationship for the studied compounds may be attributed - at least partially - to the influence of substituents on rate and directions of the metabolic transformations which occur *in vivo*.

The compound **3a**, being not toxic at 600 mg/kg, elicits quite significant anti-nociceptive effect at the dose of 15 mg/kg, above an average value for MET at the same dose. This may open an avenue for design of non-toxic structural CEL analogues *via* bulky alkyl or aromatic substitution at the oxygen in **3a** (Fig. **2**). The aromatic ring at the position 5 in CEL can be substituted while retaining significant biological activity level for corresponding derivative [63].

The analgesic property of the CF_3-AP **2a** was further assessed in the tail flick test and inflammation induced hyperalgesia model (mechanical pressure on rat paw).

In the tail flick test the anti-nociceptive effect was evaluated by measuring the latency time after application of the radian hit to the proximal third of the rat tail one and two hours after the samples injection [33]. The level of activity was estimated as percentage to the baseline value. The compound **2a** was injected in the chosen screening dose of 15 mg/kg. MET was used as a reference drug at the higher dose (163 mg/kg, which is approx. $0.05LD_{50}$) in order to ensure its analgesic action in the experiment conditions. Both CF_3-AP **2a** and MET exhibited anti-nociceptive effect one hour after the injection (Fig. **5**). After 2 h time point MET partially retained the effect ($p<0.05$ compared to control) while **2a** did not.

In the hyperalgesia test [33] an inflammatory pain was induced by carrageenan injection in the rats hind paw. A classical and effective NSAID DIF (10 mg/kg) produced significant decrease in the severity of the inflammation induced hyperalgesia: the latency time increased more than twice ($p<0.01$) compared with not-treated control. The effect of **2a** (15 mg/kg) may be described as a tendency in increasing the latency ($p<0.1$ compared to the vehicle treated control) (Fig. **5**).

4.2.6. Anti-Inflammatory Activity

The carrageenan induced hind paw edema model in rats was used for synthesized compounds anti-inflammatory activity primary evaluation [33]. The test was completed mainly with the compounds which were active in the hot plate test. The measurements of paw volume were conducted at the 1st, 3rd and 5th h after carrageenan injection.

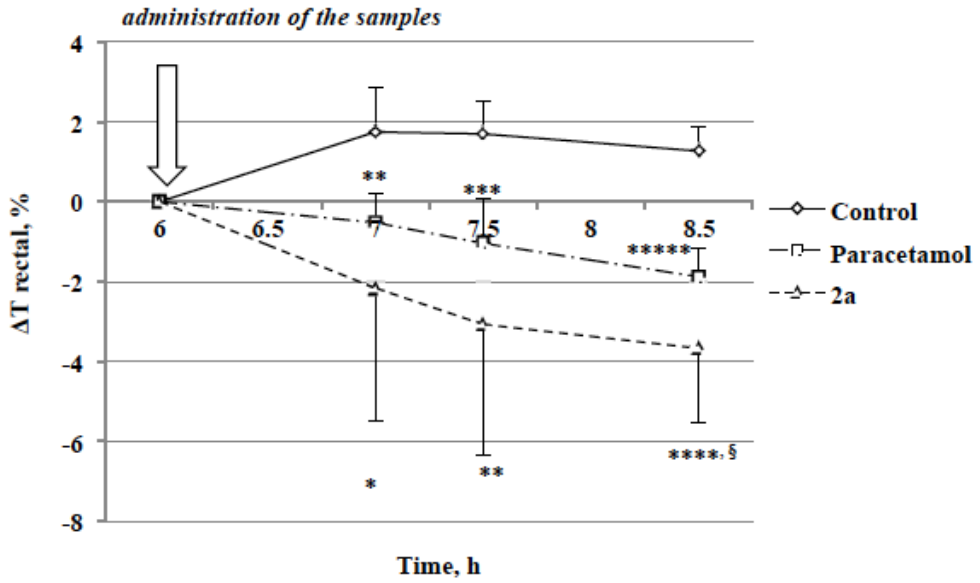

Fig. (6). Changes in rectal temperature of rats. Each point represents the mean values ± SD for 6 rats. Vehicle (control), paracetamol (100 mg/kg) and compound **2a** (30 mg/kg) were administered 6 h after the brewer's yeast injection. Temperatures were measured 60, 90 and 270 min after, Δ Trec,% calculated as it is described in the experimental section. *p < 0.05; **p < 0.01; ***p<0.001; ****p<0.0001; *****p<0.00001 compared with control; §p <0.05 compared with paracetamol.

Pre-treatment of rats with a set of the synthesized compounds and with MET at the 15 mg/kg dose did not lead to any statistically valid results with few exceptions (Table **2**). The *p*-nitrophenyl derivative **2c** (15 mg/kg) produced slight pro-inflammatory effect at the 3rd h. The CF_3-AP **2a** (15 mg/kg) exhibited anti-inflammatory activity comparable with such of DIF administered in lower dose (10 mg/kg). At the same time when **2a** was introduced in 10 mg/kg dose it appeared to be significantly less active than DIF at the same dose.

Relatively high doses of AP and propyphenazone (50 mg/kg, subcutaneously) are required in order to achieve at least mild paw edema inhibition development in the carrageenan model in mice [14]. For AP given to rats orally in the same test settings, median ED_{50} value was 432.9 mg/kg [64]. In this regard the obtained results for **2a** (more than 50% inhibition during nearly three hours after inflammation induction) look very encouraging and supporting the chosen direction of the AP structure optimization.

Thus, only CF_3-AP **2a**, being the most active in the hot plate test, elicit an anti-inflammatory effect. All the compounds with lower analgesic activity appeared not to be potent. This data may reflect the fact that even though the anti-nociceptive and anti-inflammatory properties of synthesized compounds most probably arise from modulating different sets of targets, they may partially overlap.

4.2.7. Additional CF_3-AP 2a Evaluation

According to the reported ED_{50} data, PSBDs are generally more effective fever reducers than acetylsalicylic acid and cause ulcerogenic effect at significantly higher doses than the latter [64]. Consequently, antipyretic activity would be a valid property for new pyrazolone derivatives.

Antipyretic property of the leading compound **2a** (at the dose of 30 mg/kg) was assessed in rats with fever induced by subcutaneous injection of brewer's yeast. Paracetamol was used as a reference drug at the dose of 100 mg/kg [33]. The tested compound **2a** significantly reduced the rats rectal temperature at all time points on the level of paracetamol ($p< 0.05$ if the data for both samples with control is compared) (Fig. **6**).

The tests which were used for evaluating the compounds analgesic properties, were based on the animals pain-avoiding behavioral reactions. The behavioral component interpretation may influence the outcomes of the nociceptive threshold evaluation. In order to estimate if the obtained analgesic activity data had any correlation with to the direct influence of the leading compound on the animals behavioral patterns, the open field test in mice was performed [33, 65].

The obtained data revealed that CF_3-AP **2a** at the dose of 15 mg/kg does not influence mice locomotion, anxiety and exploratory behavior. Such result supports the conclusion that compound **2a** increases the pain thresholds in the applied test systems *via* true analgesic properties.

Thus, CF_3-AP **2a** shows all of the targeted anti-inflammatory, analgesic and antipyretic effects are on the higher level than those of DIF and MET. The antipyretic for the tested compound seems to be even higher that of paracetamol.

4.3. Possible Mechanism

Lack of correlation between the *in vivo* data for synthesized compounds anti-inflammatory and analgesic activities may result from the modulating the function of biological targets distinct sets which are not completely overlapping for the two types of activity. It seems that the leading compound **2a** may successfully modulate both sets

Table 3. Molecular docking results of the pyrazoles 2, 3 into the tyrosine active site of COX-1/2.

ID Ligand[a]	COX-1 (PDB code 3N8Y)		COX-2 (PDB code 3LN1)	
	ΔG_{bind} (kcal/mol)	|LE|[b]	ΔG_{bind} (kcal/mol)	|LE|[b]
ACD	-11.56	0.52	-11.47	0.52
DIF	-10.51	0.55	-10.86	0.57
SC-560	-10.45	0.44	–	–
CEL	–	–	-12.77	0.49
2a	-9.44	0.55	-8.78	0.52
2b	-8.85	0.47	-7.84	0.44
2c	-7.52	0.38	-7.59	0.38
2d	-9.77	0.54	-7.81	0.43
2e	-9.25	0.44	-8.49	0.40
3a	-8.74	0.46	-9.06	0.53
3c	-7.27	0.36	-6.31	0.32
3e	-9.72	0.46	-9.44	0.45

[a] ID ligand correspond to Protein Data Bank; [b] Ligand efficiency ($LE = \Delta G_{bind}/N_{heavy\ atoms}$).

exhibiting anti-inflammatory, analgesic and, additionally, antipyretic effects.

This is consistent with the fact that the elucidation of pathways and targets involved in the PSBDs biological activity is still widely debated. The hypotheses vary from considering the parent compounds the major biological effects contributors [12] to almost completely attributing biological activity to its metabolites [11, 49, 50]. The list of putative targets which are involved in the pyrazolones biological effect is expanding as well.

The key prostaglandin synthesis enzymes (COX-1 and COX-2) inhibition is the main mechanism of action for traditional NSAIDs. It was believed that inhibition of COX-2 activity may be an important contributor to the PSBDs biological activity [66]. Further it was discovered that the their site of action may not involve the the enzyme active site , as the metabolic products possibly interfere with the enzyme catalytic activity initiation *via* radicals scavenging [10]. In this regard, an edaravone represents an interesting case since despite that it is structurally one of the AP's metabolites (norantipyrine) it may be partially responsible for the AP biological activity. Edaravone found to be effective when administered intrathecally to treat inflammatory-induced pain in rats but not in case of the heat induced pain in the tail flick test. Additionally, edaravone was proven to prevent the development of neuropathic pain [67, 68].

On the list of the putative targets cannabinoid system enzymes may also be found. Among the latest data there are evidences that PSBDs block the signaling pathway activated by oxidative stress by-products by stimulating the TRPA1 channel which is reviled in inflammatory and neuropathic pain models [12].

The hot plate and especially tail flick tests are considered to be very effective for centrally acting analgesic drugs efficacy and potency evaluation, while the hyperalgesia test has been proven to provide mixed results for both central and peripheral analgesics [33]. The anti-nociceptive effects produced by **2a** at the same dose of 15 mg/kg in the three pain models reflect their mechanisms of action producing different outcomes on the distinct pain induction and development paths used in these models, which supports the "multi-targetness" of this compound. The overall effective carrageenan induced edema reduction and a clear trend to produce anti-hyperalgesic activity in the Randal-Sellito test may imply the the compound **2a** or its metabolites participation in the prostaglandine synthesis inhibition [69, 70].

In order to investigate if the synthesized compounds may inhibit the COX enzymes, we carried out a molecular docking into the COX1/COX2 enzymes active sites. Two cyclooxygenase enzyme isoforms, COX-1 and COX-2 (PDB [71] codes 3N8Y [72] and 3LN1 [73]), in a complex with arachidonic acid (ACD) as native ligand and well-known COX inhibitors, DIF, SC-560 [74] and CEL, were used as the basic biological targets for estimation of tested compounds action and efficiency/selectivity. The compounds **2a-e, 3a,c,e** docking into the COX-1 and COX-2 tyrosine sites was performed and the estimated binding energy (ΔG_{bind}) as well as ligand efficiencies of these derivatives were compared with those of native ligand and COX inhibitors (Table **3**).

The ligands **2a-e, 3a,c,e** are located into the tyrosine site at the top of hydrophobic channel COX-1 near Tyr385 (Fig. **7**) and form H-bond bridges with some amino acids and π-π stacking with aromatic amino acids.

The docking scores for all compounds were ranging between -7.27 to -9.72 units in accordance to results calculated for COX-1 (Table **3**). The obtained values were higher in comparison to those of ACD and DIF. However, the **2a,d, 3a,e** ligand efficiencies were consistent with the ones of reference drug DIF (0.55). The docking scores

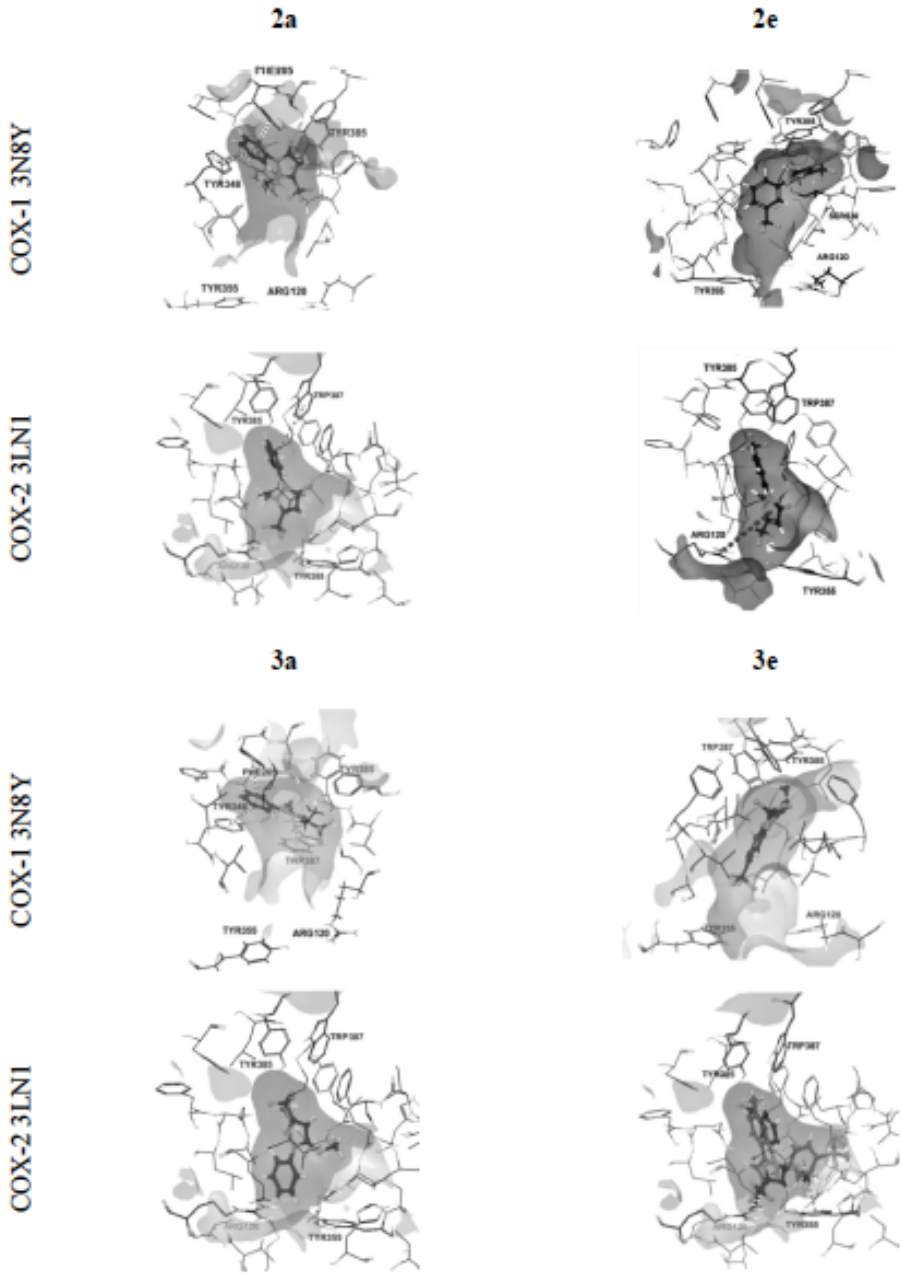

Fig. (7). The location of the compounds **2a,e, 3a,e** into the tyrosine binding site of COX-1/2: (For additional figures, please see Supplementary material).

obtained by **2a-e, 3a,c,e** docking into the COX-2 tyrosine site lie in the interval from -6.31 to -9.06 units. The COX-2 hydrophobic channel is wider than of the COX-1 one, and ligands are located in the middle of the channel near trans-membrane domain (Fig. **7**).

Calculation results confirm that COX1/2 are likely not the primary targets of the synthesized compounds. As a further step, major metabolites elucidation for **2a** would be required and their synthesis as well as biological activity evaluated.

CONCLUSION

We have developed the convenient methods for regioselective 1-aryl-3-polyfluoroalkylpyrazol-5-ols methyl-ation leading to the *N*-methylpyrazolones and *O*-methyl-pyrazoles synthesis as AP and CEL analogs respectively. For the first time the biological properties of new derivatives were confirmed *in vitro* (permeability through the biological membranes) and *in vivo* (anti-inflammatory, analgesic activities, acute toxicity). The trifluoromethyl-AP was found to be active in a full set of applied testing systems: hot plate, tail flick, mechanical hiperalgesia (Randall-Selitto), carrageenan-induced inflammation and yeast-induced pyrexia. At the same time this compound did not influence mice locomotor activity, anxiety and exploratory behavior assessed in the open field test. The trifluoromethyl-AP **2a** represents a valuable starting point in design of the lead series for new antipyretic analgesics with anti-inflammatory properties discovery.

ETHICS APPROVAL AND CONSENT TO PARTICIPATE

Not applicable.

HUMAN AND ANIMAL RIGHTS

Laboratory animals (Sprague Dawley rats and CD-mice) were obtained from the Animal Unit 'Pushino' at the M.M. Shemyakin and Yu.A. Ovchinnikov from Institute of Bioorganic Chemistry RAS (Russia). The animals were housed at natural light cycle and otherwise in a controlled environment, in propylene cages (Bioskape), on standard bedding (Rehofix MK 2000, J. Rettenmaier&Söhne, Germany), supplied with feed for conventional laboratory rodents (Chara,"Assortiment-Agro", Russia) and (ProKorm, "BioPro", Russia), water *ad libitum*. Animal care and all the procedures were performed by professional staff according to the Federal Law №61-FZ [62] and guidelines for pre-clinical study of medicinal products [34].

CONSENT FOR PUBLICATION

Not applicable.

CONFLICT OF INTEREST

The authors declare no conflict of interest, financial or otherwise.

ACKNOWLEDGEMENTS

This work was supported by the Russian Science Foundation (Grant No. 16-13-10255).

Analytical studies were carried out using equipment of the Center for Joint Use "Spectroscopy and Analysis of Organic Compounds" at the Postovsky Institute of Organic Synthesis of the Russian Academy of Sciences (Ural Branch). All calculations were carried out on a cluster in the regional centre for shared computer equipment at the Ufa Institute of Chemistry RAS (Russia).

SUPPLEMENTARY MATERIAL

Supplementary material is available on the publisher's website along with the published article.

REFERENCES

[1] Brune, K. The Early History of Non-Opioid Analgesics. *Acute Pain* **1997**, *1* (1), 33–40.

[2] Aronson, J.K. *Meyler's Side Effects of Analgesics and Anti-Inflammatory Drugs*; Elsevier Science B.V.: The Netherland, Amsterdam, **2009**.

[3] Bruera, E.D.; Portenoy, R.K. *Cancer Pain: Assessment and Management*; Cambridge University Press: New York, USA, 2009.

[4] Jasiecka, A.; Maślanka, T.; Jaroszewski, J.J. Pharmacological Characteristics of Metamizole. *Pol. J. Vet. Sci.* **2014**, *17*(1), 207–214.

[5] Kötter, T.; da Costa, B.R.; Fässler, M.; Blozik, E.; Linde, K.; Jüni, P.; Reichenbach, S.; Scherer, M. Metamizole-Associated Adverse Events: A Systematic Review and Meta-Analysis. *PLoS One* **2015**, *10*(4), e0122918.

[6] Tesfa, D.; Keisu, M.; Palmblad, J. Idiosyncratic Drug-Induced Agranulocytosis: Possible Mechanisms and Management. *Am. J. Hematol.* **2009**, *84*(7), 428–434.

[7] Watanabe, T.; Tahara, M.; Todo, S. The Novel Antioxidant Edaravone: From Bench to Bedside. *Cardiovasc. Ther.* **2008**, *26*(2), 101–114.

[8] Kikuchi, K.; Miura, N.; Kawahara, K.-I.; Murai, Y.; Morioka, M.; Lapchak, P.A.; Tanaka, E. Edaravone (Radicut), a Free Radical Scavenger, Is a Potentially Useful Addition to Thrombolytic Therapy in Patients with Acute Ischemic Stroke. *Biomed. Reports* **2013**, *1*(1), 7–12.

[9] Sawada, H. Clinical Efficacy of Edaravone for the Treatment of Amyotrophic Lateral Sclerosis. *Expert Opin. Pharmacother.* **2017**, *18*(7), 735–738.

[10] Pierre, S.C.; Schmidt, R.; Brenneis, C.; Michaelis, M.; Geisslinger, G.; Scholich, K. Inhibition of Cyclooxygenases by Dipyrone. *Br. J. Pharmacol.* **2009**, *151*(4), 494–503.

[11] Rogosch, T.; Sinning, C.; Podlewski, A.; Watzer, B.; Schlosburg, J.; Lichtman, A.H.; Cascio, M. G.; Bisogno, T.; Di Marzo, V.; Nüsing, R.; Imming P. Novel Bioactive Metabolites of Dipyrone (Metamizol). *Bioorg. Med. Chem.* **2012**, *20*(1), 101–107.

[12] Nassini, R.; Fusi, C.; Materazzi, S.; Coppi, E.; Tuccinardi, T.; Marone, I.M.; De Logu, F.; Preti, D.; Tonello, R.; Chiarugi, A.; Patacchini, R.; Geppetti, P.; Benemei, S. The TRPA1 Channel Mediates the Analgesic Action of Dipyrone and Pyrazolone Derivatives. *Br. J. Pharmacol.* **2015**, *172*(13), 3397–3411.

[13] Uramaru, N.; Shigematsu, H.; Toda, A.; Eyanagi, R.; Kitamura, S.; Ohta, S. Design, Synthesis, and Pharmacological Activity of Nonallergenic Pyrazolone-Type Antipyretic Analgesics. *J. Med. Chem.* **2010**, *53*(24), 8727–8733.

[14] Radwan, M.F.; Dalby, K.N.; Kaoud, T.S. Propyphenazone-Based Analogues as Prodrugs and Selective Cyclooxygenase-2 Inhibitors. *ACS Med. Chem. Lett.* **2014**, *5*(9), 983–988.

[15] Clark, M.P.; Laughlin, S.K.; Laufersweiler, M.J.; Bookland, R.G.; Brugel, T.A.; Golebiowski, A.; Sabat, M.P.; Townes, J.A.; VanRens, J.C.; Djung, J.F.; Natchus, M.G.; De, B.; Hsieh, L.C.; Xu, S.C.; Walter, R.L.; Mekel, M.J.; Heitmeyer, S.A.; Brown, K.K.; Juergens, K.; Taiwo, Y.O.; Janusz, M.J. Development of Orally Bioavailable Bicyclic Pyrazolones as Inhibitors of Tumor Necrosis Factor-α Production. *J. Med. Chem.* **2004**, *47*(11), 2724–2727.

[16] Liu, L.; Siegmund, A.; Xi, N.; Kaplan-Lefko, P.; Rex, K.; Chen, A.; Lin, J.; Moriguchi, J.; Berry, L.; Huang, L.; Teffera Y.; Yang Y.; Zhang Y.; Bellon, S.F.; Lee, M.; Shimanovich, R.; Bak, A.; Dominguez, C.; Norman, M.H.; Harmange, J.-C.; Dussault, I.; Kim, T.-S. Discovery of a Potent, Selective, and Orally Bioavailable c-Met Inhibitor: 1-(2-Hydroxy-2-Methylpropyl)- N -(5-(7-Methoxyquinolin-4-Yloxy)Pyridin-2-Yl)-5-Methyl-3-Oxo-2-Phenyl-2,3-Dihydro-1 H -Pyrazole-4-Carboxamide (AMG 458). *J. Med. Chem.* **2008**, *51*(13), 3688–3691.

[17] Zhou, Y.; Wang, J.; Gu, Z.; Wang, S.; Zhu, W.; Aceña, J. L.; Soloshonok, V. A.; Izawa, K.; Liu, H. Next Generation of Fluorine-Containing Pharmaceuticals, Compounds Currently in Phase II–III Clinical Trials of Major Pharmaceutical Companies: New Structural Trends and Therapeutic Areas. *Chem. Rev.* **2016**, *116*(2), 422–518.

[18] Hiyama, T.; Yamamoto, H. Biologically Active Organofluorine Compounds. In *Organofluorine Compounds*; Springer Berlin Heidelberg: Berlin, Heidelberg, **2000**; pp 137–182.

[19] *Fluorine in Medicinal Chemistry and Chemical Biology*; Ojima, I., Ed.; Wiley-Blackwell: West Sussex, UK, **2009**.

[20] Isanbor, C.; O'Hagan, D. Fluorine in Medicinal Chemistry: A Review of Anti-Cancer Agents. *J. Fluor. Chem.* **2006**, *127*(3), 303–319.

[21] Bégué, J.-P.; Bonnet-Delpon, D. Recent Advances (1995–2005) in Fluorinated Pharmaceuticals Based on Natural Products. *J. Fluor. Chem.* **2006**, *127*(8), 992–1012.

[22] Kirk, K.L. Fluorine in Medicinal Chemistry: Recent Therapeutic Applications of Fluorinated Small Molecules. *J. Fluor. Chem.* **2006**, *127*(8), 1013–1029.

[23] Hagmann, W.K. The Many Roles for Fluorine in Medicinal Chemistry. *J. Med. Chem.* **2008**, *51*(15), 4359–4369.

[24] O'Hagan, D. Fluorine in Health Care: Organofluorine Containing Blockbuster Drugs. *J. Fluor. Chem.* **2010**, *131*(11), 1071–1081.

[25] Kirsch, P. *Modern Fluoroorganic. Chemistry Synthesis, Reactivity, Applications*; WILEY-VCH Verlag GmbH & Co. KGaA, Weinheim, **2004**.

[26] Evans, T.A.; Seddon, K.R. Hydrogen Bonding in DNA—a Return to the Status Quo. *Chem. Commun.* **1997**, *21*, 2023–2024.

[27] Meyer, E.A.; Castellano, R.K.; Diederich, F. Interactions with Aromatic Rings in Chemical and Biological Recognition. *Angew. Chemie Int. Ed.* **2003**, *42*(11), 1210–1250.

[28] Shchegol'kov, E.V.; Shchur, I.V.; Burgart, Y.V.; Saloutin, V.I.; Trefilova, A.N.; Ljushina, G.A.; Solodnikov, S.Y..; Markova, L.N.; Maslova, V.V.; Krasnykh, O.P.; Borisevich, S.S.; Khursan, S.L. Polyfluorinated Salicylic Acid Derivatives as Analogs of Known Drugs: Synthesis, Molecular Docking and Biological Evaluation. *Bioorg. Med. Chem.* **2017**, *25*(1), 91–99.

[29] Djuric, S.W.; BaMaung, N.Y.; Basha, A.; Liu, H.; Luly, J. R.; Madar, D.J.; Sciotti, R.J.; Tu, N.P.; Wagenaar, F.L.; Wiedeman, P.E.; Zhou X.; Ballaron S.; Bauch J.; Chen Y.-W.; Chiou X.G.; Fey, T.; Gauvin, D.; Gubbins, E.; Hsieh, G.C.; Marsh, K.C.; Mollison, K.W.; Pong, M.; Shaughnessy, T.K.; Sheets, M.P.; Smith, M.; Trevillyan, J.M.; Warrior, U.; Wegner, C.D.; Carter, G.W. 3,5-Bis(Trifluoromethyl)Pyrazoles: A Novel Class of NFAT Transcription Factor Regulator. *J. Med. Chem.* **2000**, *43*(16), 2975–2981.

[30] Jansson, R.; Bredberg, U.; Ashton, M. Prediction of Drug Tissue to Plasma Concentration Ratios Using a Measured Volume of Distribution in Combination With Lipophilicity. *J. Pharm. Sci.* **2008**, *97*(6), 2324–2339.

[31] Cox, S.R.; Lesman, S.P.; Boucher, J.F.; Krautmann, M J.; Hummel, B.D.; Savides, M.; Marsh, S.; Fielder, A.; Stegemann, M.R. The Pharmacokinetics of Mavacoxib, a Long-Acting COX-2 Inhibitor, in Young Adult Laboratory Dogs. *J. Vet. Pharmacol. Ther.* **2010**, *33*(5), 461–470.

[32] Sheldrick, G.M. Programs for Crystal Structure Solution and Refinement. SHELXS 97 and SHELXL 97, University of Göttingen, Germany, **1997**.

[33] Vogel, H.G. *Drug Discovery and Evaluation: Pharmacological Assays*; Springer-Verlag: Berlin-Heidelberg-New York, **2008**.

[34] Mironov, A.N. *Guidelines for Pre-Clinical Study of Medicinal Products. Part One (in Russian)*; Grif&Ko: Moscow, **2012**.

[35] Kallina, C. Tail-Flick Test I: Impact of a Suprathreshold Exposure to Radiant Heat on Pain Reactivity in Rats. *Physiol. Behav.* **1995**, *58*(1), 161–168.

[36] Gainok, J.; Daniels, R.; Golembiowski, D.; Kindred, P.; Post, L.; Strickland, R.; Garrett, N. Investigation of the Anti-Inflammatory, Antinociceptive Effect of Ellagic Acid as Measured by Digital Paw Pressure via the Randall-Selitto Meter in Male Sprague- Dawley Rats. *AANA J.* **2011**, *79*(4), S28–S34.

[37] Puig, C.; Crespo, M.I.; Godessart, N.; Feixas, J.; Ibarzo, J.; Jiménez, J.-M.; Soca, L.; Cardelús, I.; Heredia, A.; Miralpeix, M.; Puig, J.; Beleta, J.; Huerta, J.M.; López, M.; Segarra, V.; Ryder, H.; Palacios, J.M. Synthesis and Biological Evaluation of 3,4-Diaryloxazolones: A New Class of Orally Active Cyclooxygenase-2 Inhibitors. *J. Med. Chem.* **2000**, *43*(2), 214–223.

[38] Pasin, J.S.M.; Ferreira, A.P.O.; Saraiva, A.L.L.; Ratzlaff, V.; Andrighetto, R.; Machado, P.; Marchesan, S.; Zanette, R.A.; Bonacorso, H.G.; Zanatta, N.; Martins, M.A.P.; Ferreira, J.; Mello, C.F. Antipyretic and Antioxidant Activities of 5-Trifluoromethyl-4,5-Dihydro-1H-Pyrazoles in Rats. *Brazilian J. Med. Biol. Res.* **2010**, *43*(12), 1193–1202.

[39] Hall, C.S. Emotional Behavior in the Rat. III. The Relationship between Emotionality and Ambulatory Activity. *J. Comp. Psychol.* **1936**, *22*(3), 345–352.

[40] Gould, T.D.; Dao, D.T.; Kovacsics, C.E. The Open Field Test. In: *Mood and Anxiety Related Phenotypes in Mice. Neuromethods*; Gould T., Ed.; Humana Press: Totowa, NJ, **2009**; Vol. 42, pp 1–20.

[41] *OECD Guideline 423: Acute Oral Toxicity. Paris: OECD* **1996**.

[42] Saloutin, V.I.; Fomin, A.N.; Pashkevich, K.I. Reaction of Fluorine-Containing b-Ketoesters with Bifunctional N-Nucleophiles. *Bull. Acad. Sci. USSR Div. Chem. Sci.* **1985**, *34*(1), 135–141.

[43] Al-Mutairi, A.A.; El-Baih, F.E.M.; Al-Hazimi, H.M. Microwave versus Ultrasound Assisted Synthesis of Some New Heterocycles Based on Pyrazolone Moiety. *J. Saudi Chem. Soc.* **2010**, *14*(3), 287–299.

[44] Hamper, B.C.; Kurtzweil, M.L.; Beck, J.P. Cyclocondensation of Alkylhydrazines and .Beta.-Substituted Acetylenic Esters: Synthesis of 3-Hydroxypyrazoles. *J. Org. Chem.* **1992**, *57*(21), 5680–5686.

[45] Chen, Z.-P.; Chen, M.-W.; Shi, L.; Yu, C.-B.; Zhou, Y.-G. Pd-Catalyzed Asymmetric Hydrogenation of Fluorinated Aromatic Pyrazol-5-Ols via Capture of Active Tautomers. *Chem. Sci.* **2015**, *6*(6), 3415–3419.

[46] Nemytova, N.A.; Shchegol'kov, E.V.; Burgart, Y.V.; Slepukhin, P.A.; Borisevich, S.S.; Khursan, S.L.; Saloutin, V.I. Regiocontrolled N-, O- and C-Methylation of 1-Phenyl-3-Polyfluoroalkyl-1H-Pyrazol-5-ols. *J. Fluor. Chem.* **2018**, *206*, 72–81.

[47] Grillot, G.; Aftergut, S.; Botteron, D. Notes - Trifluoroantipyrene. *J. Org. Chem.* **1958**, *23*(1), 119–120.

[48] Amrein, K.; Hunziker, D.; Kuhn, B.; Mayweg, A.; Neidhart, W. New pyrazolones as 11b-HSD1 inhibitors for diabetes. Patent US Patent 2,007,049,574, March 01, **2007**.

[49] Volz, M.; Kellner, H. Kinetics and Metabolism of Pyrazolones (Propyphenazone, Aminopyrine and Dipyrone). *Br. J. Clin. Pharmacol.* **1980**, *10*(S2), 299S–308S.

[50] Ariza, A.; García-Martín, E.; Salas, M.; Montañez, M.I.; Mayorga, C.; Blanca-Lopez, N.; Andreu, I.; Perkins, J.; Blanca, M.; Agúndez, J.A.G.; Torres, M.J. Pyrazolones Metabolites Are Relevant for Identifying Selective Anaphylaxis to Metamizole. *Sci. Rep.* **2016**, *6*(1), 23845.

[51] Lipinski, C.A. Lead- and Drug-like Compounds: The Rule-of-Five Revolution. *Drug Discov. Today Technol.* **2004**, *1*(4), 337–341.

[52] Mirza, A.; Desai, R.; Reynisson, J. Known Drug Space as a Metric in Exploring the Boundaries of Drug-like Chemical Space. *Eur. J. Med. Chem.* **2009**, *44*(12), 5006–5011.

[53] Small-Molecule Drug Discovery Suite 2017-4, Schrödinger, LLC, New York, NY. **2017**.

[54] Lipinski, C.A.; Lombardo, F.; Dominy, B.W.; Feeney, P.J. Experimental and Computational Approaches to Estimate Solubility and Permeability in Drug Discovery and Development Settings. *Adv. Drug Deliv. Rev.* **1997**, *23*(1–3), 3–25.

[55] Congreve, M.; Carr, R.; Murray, C.; Jhoti, H.A 'Rule of Three' for Fragment-Based Lead Discovery? *Drug Discov. Today* **2003**, *8*(19), 876–877.

[56] Kansy, M.; Senner, F.; Gubernator, K. Physicochemical High Throughput Screening: Parallel Artificial Membrane Permeation Assay in the Description of Passive Absorption Processes. *J. Med. Chem.* **1998**, *41*(7), 1007–1010.

[57] Ruell, J.A.; Avdeef, A. Absorption Screening Using the PAMPA Approach. In *Optimization in Drug Discovery*; Yan, Z.; Caldwell, G.W., Eds.; Humana Press: Totowa, NJ, **2004**; pp 37–64.

[58] Barnes-Seeman, D.; Beck, J.; Springer, C. Fluorinated Compounds in Medicinal Chemistry: Recent Applications, Synthetic Advances and Matched-Pair Analyses. *Curr. Top. Med. Chem.* **2014**, *14*(7), 855–864.

[59] Gein, V.L.; Popov, A.V.; Kolla, V.E.; Popova, N.A.; Potemkin, K.D. Synthesis and Biological Activity of 1,5-Diaryl-3-Arylamino-4-Carboxymethyl-2,5-Dihydro-2-Pyrrolones and 1,5-Diaryl-4-Carboxymethyltetrahydropyrrole-2,3-Diones. *Pharm. Chem. J.* **1993**, *27*(5), 343-346.

[60] Endel'man, E.S.; Fadeicheva, A.G.; Fialkov, Y.A.; Danilenko, V.S.; Trinus, F.P.; Chernoshtan, K.A.; Yagupol'skii, L.M. Synthesis and Study of the Biological Properties of Fluorinated Derivatives of 1-Phenyl-3-Methylpyrazol-5-One. Antipyrine Analogs with Heteroatomic Fluorine-Containing Substituents. *Khim. Farm. Zh.* **1976**, *10*(12), 27.

[61] Piskarev, A.V.; Nesterenko, V.S.; Suminov, S.I. Effect of Pyrazolone and Hydrazine Derivatives on the Resistance of Mice to Hypoxia. *Farmakol. i Toksikol.* **1973**, *36*(1), 48–54.

[62] *On Circulation of Medicines. Federal Law of 12.04.2010.№61-FZ RF*.

[63] Lu, Z.; Xiong, X.; Zhang, B.; Lin, G.; Shi, Y.; Liu, Z.; Meng, J.; Zhou, Y.; Mei, Q. Evaluation of 2 Celecoxib Derivatives: Analgesic Effect and Selectivity to Cyclooxygenase-2/11. *Acta Pharmacol. Sin.* **2005**, *26*(12), 1505–1511.

[64] Romer, D. Pharmacological Evaluation of Mild Analgesics. *Br. J. Clin. Pharmacol.* **1980**, *10*(S2), 247S–251S.

[65] Buccafusco, J.J. *Methods of Behavior Analysis in Neuroscience, 2nd Edition*; CRC Press, Taylor & Francis: Boca Rato, FL, **2009**.

[66] Campos, C.; de Gregorio, R.; García-Nieto, R.; Gago, F.; Ortiz, P.; Alemany, S. Regulation of Cyclooxygenase Activity by Metamizol. *Eur. J. Pharmacol.* **1999**, *378*(3), 339–347.

[67] Nishiyama, T.; Ogawa, M. Intrathecal Edaravone, a Free Radical Scavenger, Is Effective on Inflammatory-Induced Pain in Rats. *Acta Anaesthesiol. Scand.* **2005**, *49*(2), 147–151.

[68] Mao, Y.-F.; Yan, N.; Xu, H.; Sun, J.-H.; Xiong, Y.-C.; Deng, X.-M. Edaravone, a Free Radical Scavenger, Is Effective on Neuropathic Pain in Rats. *Brain Res.* **2009**, *1248*, 68–75.

[69] Nantel, F.; Denis, D.; Gordon, R.; Northey, A.; Cirino, M.; Metters, K.M.; Chan, C.C. Distribution and Regulation of Cyclooxygenase-2 in Carrageenan-Induced Inflammation. *Br. J. Pharmacol.* **1999**, *128*(4), 853–859.

[70] Guay, J.; Bateman, K.; Gordon, R.; Mancini, J.; Riendeau, D. Carrageenan-Induced Paw Edema in Rat Elicits a Predominant Prostaglandin E 2 (PGE 2) Response in the Central Nervous System Associated with the Induction of Microsomal PGE 2 Synthase-1. *J. Biol. Chem.* **2004**, *279*(23), 24866–24872.

[71] Berman, H.M.; Westbrook, J.; Feng, Z.; Gilliland, G.; Bhat, T.N.; Weissig, H.; Shindyalov, I.N.; Bourne, P.E. The Protein Data Bank. *Nucleic Acids Res.* **2000**, *28*(1), 235–242.

[72] Sidhu, R.S.; Lee, J.Y.; Yuan, C.; Smith, W.L. Comparison of Cyclooxygenase-1 Crystal Structures: Cross-Talk between Monomers Comprising Cyclooxygenase-1 Homodimers,. *Biochemistry* **2010**, *49*(33), 7069–7079.

[73] Wang, J.L.; Limburg, D.; Graneto, M.J.; Springer, J.; Hamper, J. R.B.; Liao, S.; Pawlitz, J.L.; Kurumbail, R.G.; Maziasz, T.; Talley, J.J.; Kiefer, J.R., Carter, J. The Novel Benzopyran Class of Selective Cyclooxygenase-2 Inhibitors. Part 2: The Second Clinical Candidate Having a Shorter and Favorable Human Half-Life. *Bioorg. Med. Chem. Lett*. **2010**, *20*(23), 7159–7163.

[74] Smith, C.J.; Zhang, Y.; Koboldt, C.M.; Muhammad, J.; Zweifel, B.S.; Shaffer, A.; Talley, J.J.; Masferrer, J.L.; Seibert, K.; Isakson, P.C. Pharmacological Analysis of Cyclooxygenase-1 in Inflammation. *Proc. Natl. Acad. Sci.* **1998**, *95*(22), 13313–13318.